

---

# NeFL: Nested Federated Learning for Heterogeneous Clients

---

**Honggu Kang**  
KAIST  
khg13@kaist.ac.kr

**Seohyeon Cha**  
KAIST  
kaitjgus@kaist.ac.kr

**Jinwoo Shin**  
KAIST  
jinwoos@kaist.ac.kr

**Jongmyeong Lee**  
KAIST  
whenstyle07@kaist.ac.kr

**Joonhyuk Kang**  
KAIST  
jkang@kaist.ac.kr

## Abstract

Federated learning (FL) is a promising approach in distributed learning keeping privacy. However, during the training pipeline of FL, slow or incapable clients (i.e., stragglers) slow down the total training time and degrade performance. System heterogeneity, including heterogeneous computing and network bandwidth, has been addressed to mitigate the impact of stragglers. Previous studies split models to tackle the issue, but with less degree-of-freedom in terms of model architecture. We propose *nested federated learning (NeFL)*, a generalized framework that efficiently divides a model into submodels using both depthwise and widthwise scaling. NeFL is implemented by interpreting models as solving ordinary differential equations (ODEs) with adaptive step sizes. To address the *inconsistency* that arises when training multiple submodels with different architecture, we decouple a few parameters. NeFL enables resource-constrained clients to effectively join the FL pipeline and the model to be trained with a larger amount of data. Through a series of experiments, we demonstrate that NeFL leads to significant gains, especially for the worst-case submodel (e.g., **8.33%** improvement on CIFAR-10). Furthermore, we demonstrate NeFL aligns with recent studies in FL.

## 1 Introduction

The success of deep learning owes much to large-scale computing infrastructures and vast amounts of training data where a large amount of data comes from mobile devices and internet-of-things (IoT) devices. Recently, privacy regulations regarding data collection have gained attention, potentially impeding development [1, 17]. A distributed machine learning framework, federated learning (FL) is getting attention to address the privacy concerns. FL enables model training by collaboratively leveraging the vast amount of data on clients while preserving data privacy. Rather than centralizing raw data, FL collects trained model weights from clients, which are aggregated on a server by a method (e.g., FedAvg) [49]. FL has shown its potential, and several studies have explored to utilize it more practically [43, 28, 44, 22, 20, 48, 71, 24, 29, 33].

Despite the promising perspective, FL faces challenges of systems-related heterogeneity [32, 40]. Clients with heterogeneous resources, such as computing power, communication bandwidth, and memory, introduce stragglers that lead to longer delays and training times during the FL pipeline. The FL server must make decisions on whether to wait for or drop out stragglers. The exclusion of stragglers can result in performance degradation, such as reduced prediction accuracy. Therefore, FL must accommodate clients with heterogeneous resources. Mobile and embedded devices, with their limited memory, storage, and network bandwidth, often struggle when training a large model. These

resource-poor clients risk becoming stragglers, leading to a biased model trained predominantly on data from resource-rich clients. Otherwise, reducing the global model size to accommodate poor clients can degrade performance due to limited model capacity. To this end, FL with a single global model may not be efficient for heterogeneous clients.

In this paper, we propose *Nested Federated Learning (NeFL)*, a method that embraces existing studies of federated learning in a nested manner [29, 15, 33]. While FL trains a model with a fixed size and structure, NeFL trains several submodels of adaptive sizes to meet clients' dynamic requirements (e.g., memory, computing and bandwidth dynamics). We propose to scale down model into submodels generally (by widthwise or/and depthwise). The scaling is motivated by interpreting a model forwarding as solving ordinary differential equations (ODEs). The interpretation also motivated us to propose the submodels to have *learnable step size parameters* and the concept of *inconsistency*. The scaling method provides more degree-of-freedom (DoF) to scale down a model than previous studies [29, 15, 33]. The increased DoF make submodels to be more efficient in size [59] and provides more flexibility on model size and computing cost. We also propose a parameter averaging method for NeFL: *Nested Federated Averaging (NeFedAvg)* for averaging *consistent parameters* and FedAvg for averaging *inconsistent parameters* of submodels. Notably, NeFL outperforms the Top-1 accuracy of baselines by **8.33%** for the worst-case submodel of ResNet110.

Additionally, we verify if NeFL aligns with the recently proposed ideas in FL: (i) pre-trained models improve the performance of FL in both identically independently distributed (IID) and non-IID settings [9] and (ii) simply rethinking the model architecture improves the performance, especially in non-IID settings [53]. We observe that NeFL with ViTs shows **22.7%** better performance than previous widthwise scaling based method with ViTs for IID dataset and **24.49%** for non-IID dataset with submodel employing 50% parameters of a global model (to be revised into worst-case or average performance). Through a series of experiments we observe that NeFL outperforms baselines sharing the advantages of recent studies.

The main contributions of this study can be summarized as follows:

- We propose a general model scaling method employing the concept of ODE solver to deal with the system heterogeneity.
- We propose a parameter averaging method of the generally scaled submodels by NeFedAvg and FedAvg.
- We evaluate the performance of NeFL through a series of experiments and verify the applicability of NeFL over recent studies.

## 2 Related Works

**Knowledge distillation** Knowledge distillation (KD) aims to compress models by transferring knowledge from a large teacher model to a smaller student model [27]. Several studies have explored the integration of knowledge distillation within the context of federated learning [57, 64, 4, 44, 70, 23]. These studies investigate the use of KD to address (i) reducing the model size and communication bottleneck associated with transmitting model weights and (ii) fusing the knowledge of several models with different architectures. FedKD [64] proposes an adaptive mutual distillation where distillation is controlled based on prediction performance. FedGKT [23] presents a edge-computing method that employs knowledge distillation to train resource-constrained devices. The method partitions the model, and clients transfer intermediate features to an offloading server for task offloading. FedDF [44] introduces a model fusion technique that employs ensemble distillation to combine models with different architecture. However, it is worth noting that knowledge distillation-based FL requires shared data or shared generative models to get the knowledge distillation loss. Alternatively, clients can transfer trained models to the other clients [4].

**Compression and sparsification** Several studies have focused to deal with the communication bottleneck [54, 20]. The literature studies gradient compression (e.g., quantization or sparsification) and reducing communication rounds [20]. FetchSGD [54] proposes a method that compresses model updates using a Count Sketch and merge them. Some approaches aim to represent the weights of a larger network using a smaller network [19, 7]. However, these studies primarily address heterogeneous communication bandwidth. Pruning is another technique that can be used to

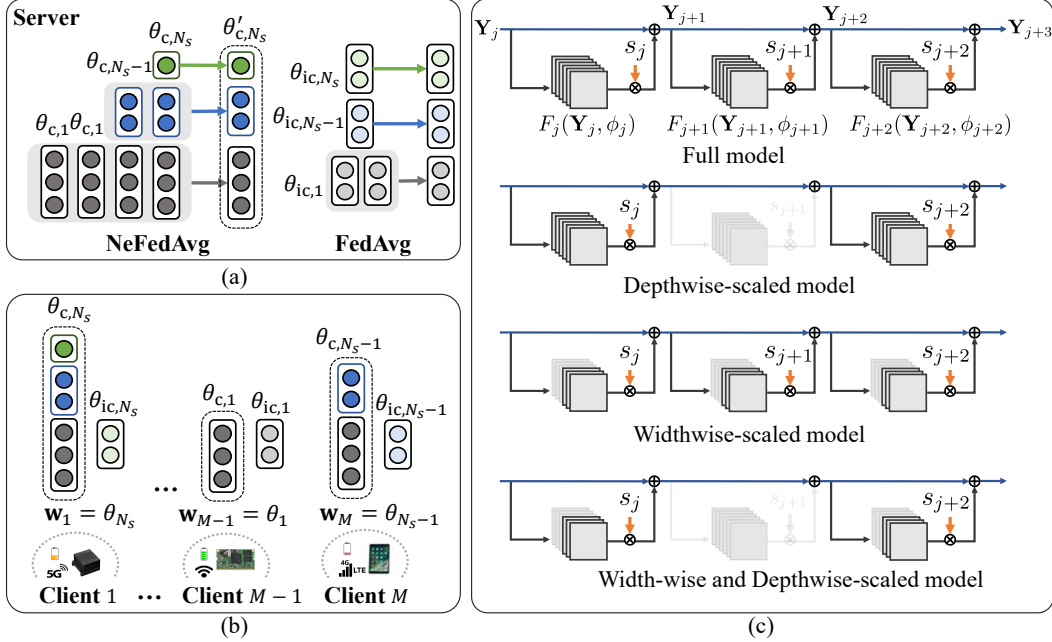


Figure 1: **FL with generally split submodels.** NeFL aggregates weights of submodels, where the submodels are scaled by both widthwise and depthwise. The weights include consistent and inconsistent parameters.

compress models. However, it typically determines the submodel based on the worst case of resource-constrained clients, which means it does not fully leverage the capabilities of the resource-rich clients [36, 31, 50].

**Dynamic runtime** The concept of interpreting neural networks with residual connections as numerically solving ODEs was introduced in NeuralODE [10]. By using numerical techniques such as computing with less steps, the ODE can be solved with reduced computational requirements. Otherwise, with more computing, the ODE can be solved achieving less numerical errors [21]. This approach offers a way to dynamically optimize computation. Split learning [62, 60, 23] is another technique that addresses the issue of resource-constrained clients by leveraging richer computing resources, such as cloud or edge servers. The methods provide solutions for clients with heterogeneous computing power or runtime dynamics. However, these methods primarily studies on improving the efficiency of resource allocation or computational distribution, rather than explicitly addressing system heterogeneity.

**Model splitting** Various approaches have been proposed to address the heterogeneity of clients by splitting the global network based on their capabilities [29, 15, 33]. LG-FedAvg [43] introduced a method to split the model and decouple the layers into global and local layers, reducing the number of parameters that need to be communicated. While FjORD [29] and HeteroFL [15] split a global model widthwise, DepthFL [33] split a global model depthwise. Unlike widthwise scaling, DepthFL incorporates an additional bottleneck layer and an independent classifier for every submodel. However, it has been observed that *deep and narrow* models as well as *shallow and wide* models may result in inefficient performance in terms of the number of parameters or floating-point operations (FLOPs). Prior studies have shown that carefully balancing the depth and width of a network can lead to improved performance [67, 59]. Therefore, a balanced network is expected to contribute to performance gains in the context of FL.

### 3 Background

We propose to scale down the models inspired by solving ODEs in a numerical way (e.g., Euler method). Modern deep neural networks stack residual blocks that contain identity skip-connections

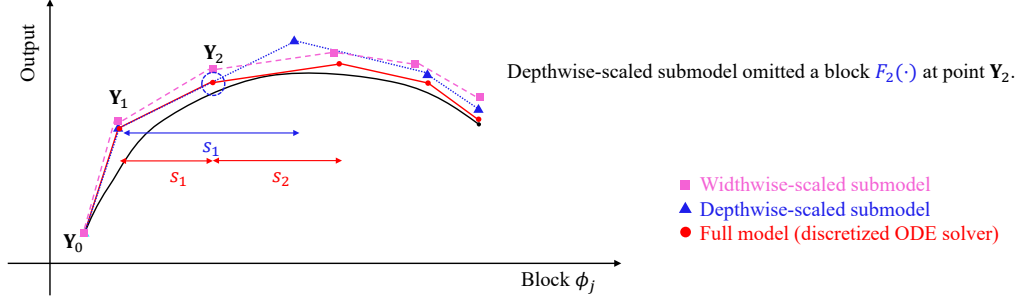


Figure 2: Model scaling inspired by ODE solver

that bypass the residual layers. A residual block is written as  $\mathbf{Y}_{j+1} = \mathbf{Y}_j + F_j(\mathbf{Y}_j, \phi_j)$ , where  $\mathbf{Y}_j$  is the feature map at the  $j$ th layer,  $\phi_j$  denotes the  $j$ th block's network parameters, and  $F_j$  represents a residual module of the  $j$ th block. These networks can be interpreted as solving ODEs by numerical analysis [8, 25].

Consider an initial value problem to find  $y$  at  $t$  given  $\frac{dy}{dt} = f(t, y)$  and  $y(t_0) = y_0$ . We can obtain  $y$  at any point by integration:  $y = y_0 + \int_{t_0}^t f(t, y)dt$ . It can be approximated by Taylor's expansion as  $y = y_0 + f(t_0, y_0)(t - t_0)$  and it can also be approximated with more steps as follows:

$$y_{n+1} = y_n + hf(t_n, y_n) = y_0 + hf(t_0, y_0) + \dots + hf(t_{n-1}, y_{n-1}) + hf(t_n, y_n), \quad (1)$$

where  $h$  denotes the step size. An ODE solver can design to compute less steps with larger step size for example as follows:  $y_{n+1} = y_0 + 2hf(t_0, y_0) + \dots + 2hf(t_{n-1}, y_{n-1})$  when  $n$  is odd. The results would be numerically less accurate than fully computing with a smaller step size. Note that the equation looks like the equation of residual connections. An output of a residual block is rewritten as follows:

$$\mathbf{Y}_{j+1} = \mathbf{Y}_j + F_j(\mathbf{Y}_j, \phi_j) = \mathbf{Y}_0 + F_0(\mathbf{Y}_0, \phi_0) + \dots + F_{j-1}(\mathbf{Y}_{j-1}, \phi_{j-1}) + F_j(\mathbf{Y}_j, \phi_j). \quad (2)$$

Motivated by interpreting the neural networks as solving ODEs, we proposed that few residual blocks can be omitted during forward propagation. For example,  $\mathbf{Y}_3 = \mathbf{Y}_0 + F_0 + F_1 + F_2$  could be approximated by  $\mathbf{Y}_3 = \mathbf{Y}_0 + F_0 + 2F_1$  omitting the  $F_2$  block. Here, we also propose *learnable step size parameters* [61, 6]. Instead of pre-determining the step size parameters ( $h$ 's in the equation 1), we let step size parameters be trained with the network parameters. For example, omitting  $F_2$  block,  $\mathbf{Y}_3 = \mathbf{Y}_0 + s_0F_0 + s_1F_1$  where  $s_i$ 's are also optimized. We scale the network by this ODE interpretation. Furthermore, it is possible to scale each residual block by adjusting its width (e.g., the size of filters in convolutional layers). The theoretical background behind width-wise scaling is provided by the Eckart-Young-Mirsky theorem [18]. A width-wise scaled residual block represents the optimal  $k$ -rank approximation of the original (full) block [29].

Referring to Figure 2, the black line represents the function to approximate, while the red line represents a discretized ode solver that is a full neural network model. The blue color line represents the depthwise-scaled submodel. The model omitted to compute block  $F_2(\cdot)$  at the point  $\mathbf{Y}_2$  and instead, larger step size for computing  $F_1(\mathbf{Y}_1, \phi_1)$  can compensate the omitted block [8]. The pink colored line that represents the widthwise-scaled submodel. Following the theorem that a model of less parameters are approximation of the a model of more parameters [18], a widthwise scaled model with fewer parameters for each block outputs a result, but with numerical error.

## 4 NeFL: Nested Federated Learning

*NeFL* implements FL that accomodate resource-poor clients. Instead of requiring every client to train a single global model, NeFL allows resource-poor clients to train submodels that are scaled in both widthwise and depthwise, based on the dynamic nature of their environments. This flexibility enables more clients, even with constrained resources, to participate in the FL pipeline, thereby providing the model with a larger and more diverse dataset. In the NeFL pipeline, heterogeneous clients have the ability to determine their submodel every iteration, allowing them to adapt to varying computing or communication bottlenecks in their respective environments. The NeFL server then aggregates the

---

**Algorithm 1** NeFL: Nested Federated Learning

---

**Input:** Submodels  $\{\mathbf{F}_k\}_{k=1}^{N_s}$ , total communication round  $T$ , the number of local epochs  $E$

- 1: **for**  $t \leftarrow 0$  to  $T - 1$  **do** // Global iterations
- 2:   NeFL server broadcasts the weights  $\{\theta_{c,N_s}, \theta_{ic,1}, \dots, \theta_{ic,N_s}\}$  to clients in  $\mathcal{C}_t$
- 3:    $\mathbf{w}_i \leftarrow \theta_j \in \{\theta_1, \dots, \theta_{N_s}\} \forall i \in \mathcal{C}_t$
- 4:   **for**  $k \leftarrow 0$  to  $E - 1$  **do** // Local iterations
- 5:     Client  $i$  updates  $\mathbf{w}_i \forall i \in \mathcal{C}_t$
- 6:   Client  $i$  transmits the weights  $\mathbf{w}_i$  to the NeFL server  $\forall i \in \mathcal{C}_t$
- 7:    $\{\theta_{c,N_s}, \theta_{ic,1}, \dots, \theta_{ic,N_s}\} \leftarrow \text{ParameterAverage}(\{\mathbf{w}_i\}_{i \in \mathcal{C}_t})$

▷ Algorithm 2

---

parameters from these different submodels, resulting in a collaborative and comprehensive model. Furthermore, during test time, clients have the flexibility to select an appropriate submodel based on their specific background process burdens, such as runtime memory constraints or CPU/GPU bandwidth dynamics. This allows clients to balance between performance and factors like memory usage or latency, tailoring to their individual needs and constraints. To this end, NeFL consists of method for scaling a model into submodels and aggregating the parameters of submodels.

NeFL scales a global model  $\mathbf{F}_G$  into  $N_s$  submodels  $\mathbf{F}_1, \dots, \mathbf{F}_{N_s}$  with corresponding weights  $\theta_1, \dots, \theta_{N_s}$ . Without loss of generality, we suppose  $\mathbf{F}_G = \mathbf{F}_{N_s}$ . The scaling method is described in following Section 4.1. During each communication round  $t$ , the clients in subset  $\mathcal{C}_t$  (which is subset of  $M$  clients) train one of the  $N_s$  submodels based on their respective environments by the local epochs  $E$ . Then, clients transmit their trained weights  $\{\mathbf{w}_i\}_{i \in \mathcal{C}_t}$  to the NeFL server which aggregates them into  $\{\theta_{c,N_s}, \theta_{ic,1}, \dots, \theta_{ic,N_s}\}$  where  $\theta_{c,k}$  and  $\theta_{ic,k}$  denote *consistent* and *inconsistent* parameters of a submodel  $k$ . The aggregated weights are then distributed to the clients in  $\mathcal{C}_{t+1}$ , and this process continues for the total number of communication rounds.

## 4.1 Model Scaling

We propose a global network slimming method which is a combined method combined of widthwise scaling and depthwise scaling. We scale the model widthwise by ratio of  $\gamma_W$  and depthwise by ratio of  $\gamma_D$ . For example, a global model is represented as  $\gamma = \gamma_W \gamma_D = 1$  and a submodel that has 25% parameters of a global model can be scaled by  $\gamma_W = 0.5$  and  $\gamma_D = 0.5$ . Unless otherwise indicated, we split the model by  $\gamma_W = \gamma_D$  [59]. We empirically observed that comparatively shallow and wide models are better to employ widthwise splitting while deep and narrow models are better to employ depthwise splitting for from-the-scratch training. Furthermore, flexible widthwise/depthwise scaling provide more degree of freedom to split the models. We further describe on the slimming strategies in following sections.

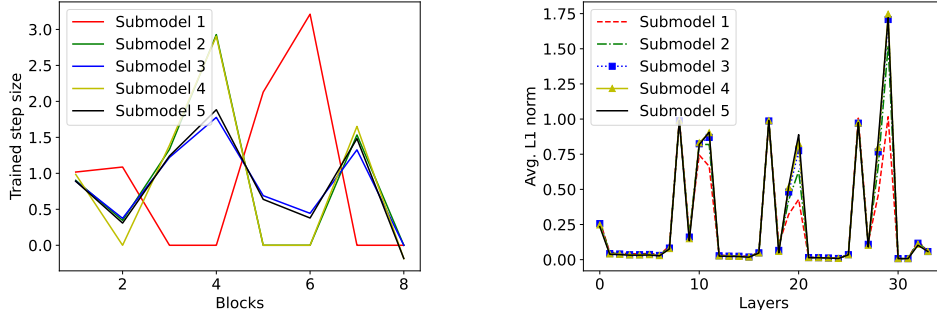
### 4.1.1 Depthwise Scaling

Residual networks, such as ResNets [25] and ViTs [16], have gained popularity due to their ability to train *deep* networks with significant performance improvements. The output of a residual block can be seen as a function multiplied by a step size as  $\mathbf{Y}_{j+1} = \mathbf{Y}_j + s_j F(\mathbf{Y}_j, \phi_j) = \mathbf{Y}_0 + \sum_j s_j F(\mathbf{Y}_j, \phi_j)$ . Note that ViTs forwards with skip connections using either self-attention (SA) layers or feed-forward networks (FFN) that  $F$  could be either SA or FFN:

$$\mathbf{Y}_{j+1} = \mathbf{Y}_j + s_j SA(\mathbf{Y}_j, \phi_j), \quad \mathbf{Y}_{j+2} = \mathbf{Y}_{j+1} + s_{j+1} FFN(\mathbf{Y}_{j+1}, \phi_{j+1}). \quad (3)$$

For example, ResNets (e.g., ResNet18, ResNet34) have a downsampling layer at the first and following residual blocks have two convolutional layers respectively and ViTs let embedding patches input into following transformer encoder blocks. ResNet34 having 16 residual blocks or ViT/B-16 have 12 encoder blocks and depthwise scaling can be implemented by skipping any of these blocks. Each block could have different number of the parameters or computing cost that it could be designed for modeling a submodel. We can observe that skipping a few blocks in a network still allows it to operate effectively [8]. This observation is in line with the concept of stochastic depth proposed in [30], where a subset of blocks is randomly bypassed during training and the all of the blocks are used during testing.

The step size parameters  $s$ 's can be viewed as dynamically training how much forward pass should be made at each step. They allow each block to adaptively contribute useful representations, and



(a) The trained submodels have different step sizes. (b) Average L1 norm of weights of submodels trained.

Figure 3: Weights of trained five submodels by NeFL

larger step sizes are multiplied to blocks that provide valuable information. Referring to Figure ?? and numerical analysis methods (e.g., Euler method, Runge-Kutta methods [21]), we can observe that adaptive step sizes, rather than uniformly spaced steps, can effectively reduce numerical errors. *Note that DepthFL [33] is a special case of the proposed depthwise scaling.*<sup>1</sup>

#### 4.1.2 Widthwise Scaling

Previous studies have been conducted on reducing the model size in the width dimension [37, 45]. In the context of NeFL, widthwise scaling is employed to slim down the network by utilizing structured contiguous pruning (ordered dropout in [29]) along with learnable step sizes. We apply contiguous channel-based pruning for convolutional networks [26] and node removal for fully connected layers. The parameters of narrow-width submodel constitute a subset of the parameters of the wide-width model. Consequently, parameters of the slimmest model are trained by every client while the parameters of the larger model is trained less frequently. This approach ensures that the parameters of the slimmest model capture the most useful representations.

We can obtain the further insights by toy example. Suppose a neural network that is linearly represented and data from a uniform distribution are given. Then, widthwise-scaled optimal submodel is the best  $k$ -rank approximation by Eckart–Young–Mirsky theorem [29, 18]. Figure 3b presents the L1 norm of weights averaged by the number of weights at each layer of five submodels [37]. (Details would be added). We observe that L1-norm averaged by the number of weights are large enough for submodel 1 (the slimmest model) and shows the slight difference with wider submodels. The slimmest model might have learned the most useful representation and the additional parameters for larger model still gets less useful information.

#### 4.2 Parameter Averaging

**Inconsistency** NeFL enables training several submodels on local data for subsequent aggregation. However, submodels of different model architectures (i.e., different width and depth) have different characteristics [3, 11, 41, 56]. Referring to Figure 2, depthwise-scaled submodel omitted to compute a block can be compensated by near steps and widthwise-scaled submodel can have different step sizes to compensate for the numerical error. We can infer that each submodel requires different step sizes to compensate for the numerical errors according to its respective model architecture. Furthermore, submodels with different model architectures have different loss landscapes. Consider the situation where losses are differentiable. A stationary point of a global model is not necessarily the stationary points of individual submodels [3, 41]. The trainability of neural networks, which varies based on network architecture, may lead the averaged submodels to become non-stationary and deviate from the optima.

<sup>1</sup>As a baseline, we implemented DepthFL without auxiliary bottleneck layers and self-distillation and implemented by pruning depthwise non-contiguously for fair comparison and ablation study that provides insights. The details are described in the Appendix.

---

**Algorithm 2** ParameterAverage

---

**Input:** Trained weights from clients  $\mathbf{W} = \{\mathbf{w}_i\}_{i \in \mathcal{C}_t}$

```
1: for  $k$  in  $\{1, \dots, N_s\}$  do
2:    $\mathcal{M}_k \leftarrow \{\mathbf{w}_i | \mathbf{w}_i = \theta_k\}_{i \in \mathcal{C}_t}$ 
3: for block  $\phi_j$  in  $\theta_{c, N_s}$  do // NeFedAvg ▷ Consistent parameters
4:    $\mathcal{M}' \leftarrow \mathcal{M} = \{\mathcal{M}_k\}_{k=1}^{N_s}$ 
5:   for  $k$  in  $\{1, \dots, N_s\}$  do
6:      $\mathcal{M}' \leftarrow \mathcal{M}' \setminus \mathcal{M}_k$  if  $\phi_j \notin \theta_{c, k}$ 
7:      $k' \leftarrow 0$ 
8:     for  $k$  in  $\{k | \mathcal{M}_k \in \mathcal{M}'\}$  do
9:        $\phi_{j, k} \setminus \phi_{j, k'} \leftarrow \sum_{\{i | \mathbf{w}_i \in \bigcup_{l \geq k, \mathcal{M}_l \in \mathcal{M}'} \mathcal{M}_l\}} \phi_{j, k}^i \setminus \phi_{j, k'}^i / \sum_{l \geq k, \mathcal{M}_l \in \mathcal{M}'} |\mathcal{M}_l|$ 
10:       $k' \leftarrow k$ 
11:  $\theta_{c, N_s} \leftarrow \bigcup_j \phi_j$ 
12: for  $k$  in  $\{1, \dots, N_s\}$  do // FedAvg [49] ▷ Inconsistent parameters
13:    $\theta_{ic, k} \leftarrow \sum_{\{i | \mathbf{w}_i \in \mathcal{M}_k\}} \theta_{ic, k}^i / |\mathcal{M}_k|$ 
```

---

The motivation led us to introduce decoupled set of parameters [43, 5] for respective submodels that require different parameter averaging method. We refer to these different characteristics between submodels as *inconsistency*. To this end, we proposed the concept of separating a few parameters, referred to as *inconsistent parameters*, from individual submodels. We addressed step size parameters and batch normalization layers as inconsistent parameters. Note that the batch normalization can improve Lipschitzness of loss, which is sensitive to the convergence of FL [56, 42]. We further provided an ablation study to assess the effectiveness of inconsistent parameters.

Meanwhile, *consistent parameters* are averaged across submodels. However, the weights of submodels are subset of the largest submodel that should be addressed differently with conventional FL. The parameters of the submodel are denoted as  $\theta_1 = \{\theta_{c, 1}, \theta_{ic, 1}\}, \dots, \theta_{N_s} = \{\theta_{c, N_s}, \theta_{ic, N_s}\}$  where  $\theta_c$  denotes consistent parameters and  $\theta_{ic}$  denotes inconsistent parameters. Note that the global parameters, which are broadcasted to clients for the next FL iteration, encompass  $\theta_{c, 1}, \theta_{ic, 1}, \dots, \theta_{ic, N_s}$ .

**Parameter Averaging** For averaging the uploaded parameters of submodels from clients, we propose Algorithm 2. Locally trained weights  $\mathbf{W} = \{\mathbf{w}_i\}_{i \in \mathcal{C}_t}$  from clients are provided as input. The NeFL server sorts the uploaded weights from clients by submodels in  $\mathcal{M}$  where  $\mathcal{M} = \{\mathcal{M}_1, \dots, \mathcal{M}_{N_s}\}$  is set of uploaded weights sorted by submodels. For consistent parameters, the parameters are averaged by *Nested Federated Averaging (NeFedAvg)*. In short, parameters are averaged by parameters that are updated in a nested manner at each client. For nested averaging of parameters, the server accesses parameters block by block. For each block, the server checks which submodel has the block (line 6 in Algorithm 2). Then, parameters are averaged in a nested manner by width. The parameters of a block with the smallest width are included in the parameters of a block with larger width. Hence, the parameters are averaged by weights of clients whose submodels have the block. Meanwhile, the parameters of a block with the largest width is only contained in a submodel that has the largest width. Thus, the parameters are averaged by clients whose submodels have the block with the largest width. Then, FedAvg [49] is employed for averaging inconsistent parameters. Each submodel has the same size of inconsistent parameters that the inconsistent parameters are averaged for respective submodels.

Consider an example with five submodels. Let us suppose that a convolutional layer from the first block is included in submodel 1, 3, and 5. Assume that submodel 1 and submodel 5 are trained twice (selected by two clients), while submodel 3 is trained three times at a communication round. Then, we have  $|\mathcal{M}_2| = |\mathcal{M}_4| = 0$ ,  $|\mathcal{M}_1| = |\mathcal{M}_5| = 2$ , and  $|\mathcal{M}_3| = 3$ . Now, delving into the parameter averaging process, the parameters exclusive to submodel 5 ( $\phi_{1, 5} \setminus \phi_{1, 3}$ ) are averaged using two updated weights ( $\mathcal{M}_5$ ). Likewise, the parameters possessed by submodel 3 but not by submodel 1 ( $\phi_{1, 3} \setminus \phi_{1, 1}$ ) are averaged using five weights ( $\mathcal{M}_5 \cup \mathcal{M}_3$ ). Finally, the parameters of submodel 1 ( $\phi_{1, 1}$ ), that is trained seven times, are averaged using seven weights ( $\mathcal{M}_5 \cup \mathcal{M}_3 \cup \mathcal{M}_1$ ). This approach ensures that consistent parameters are appropriately averaged, taking into account their depthwise inclusion and the widthwise number of occurrences across different submodels.

Table 1: Results of NeFL with five submodels for CIFAR-10 dataset under **IID** settings. We report Top-1 classification accuracies (%) for the worst-case submodel and the average of the performance of five submodels.

Model	Method	Model size	
		Worst	Avg
ResNet18	HeteroFL [15]	80.62	84.26
	FjORD [29]	85.12	87.32
	DepthFL [33]	64.80	82.44
	<b>NeFL (ours)</b>	<b>86.86</b>	<b>87.88</b>
ResNet34	HeteroFL [15]	79.51	83.16
	FjORD [29]	85.12	87.36
	DepthFL [33]	25.73	75.30
	<b>NeFL (ours)</b>	<b>87.71</b>	<b>89.02</b>

Model	Method	Model size	
		Worst	Avg
Pre-trained ResNet18	HeteroFL [15]	78.26	84.06
	FjORD [29]	86.37	88.91
	DepthFL [33]	47.76	82.86
	<b>NeFL (ours)</b>	<b>88.61</b>	<b>89.6</b>
Pre-trained ResNet34	HeteroFL [15]	79.97	84.34
	FjORD [29]	87.08	89.37
	DepthFL [33]	52.08	83.63
	<b>NeFL (ours)</b>	<b>88.36</b>	<b>91.14</b>

Table 2: Results of NeFL with five submodels for CIFAR-10 dataset under **non-IID** settings. We report Top-1 classification accuracies (%) for the worst-case submodel and the average of the performance of five submodels.

Model	Method	Model size	
		Worst	Avg
ResNet18	HeteroFL [15]	76.25	80.11
	FjORD [29]	75.81	77.99
	DepthFL [33]	59.61	76.89
	<b>NeFL (ours)</b>	<b>81.26</b>	<b>81.71</b>
ResNet34	HeteroFL [15]	76.03	79.63
	FjORD [29]	74.70	76.01
	DepthFL [33]	30.42	70.76
	<b>NeFL (ours)</b>	<b>80.76</b>	<b>83.31</b>

Model	Method	Model size	
		Worst	Avg
Pre-trained ResNet18	HeteroFL [15]	71.95	76.17
	FjORD [29]	81.81	81.96
	DepthFL [33]	39.78	67.71
	<b>NeFL (ours)</b>	<b>82.91</b>	<b>85.85</b>
Pre-trained ResNet34	HeteroFL [15]	72.33	78.2
	FjORD [29]	78.2	78.89
	DepthFL [33]	42.09	79.86
	<b>NeFL (ours)</b>	<b>83.62</b>	<b>86.48</b>

## 5 Experiment

In this section, we demonstrate the performance of our proposed NeFL over baselines. We provide the experiment results of NeFL that trains submodels from scratch. We also demonstrate whether NeFL aligns with the recently proposed ideas in FL [9, 53]: experiments that verify (i) the performance of NeFL with initial weights loaded from pre-trained model and (ii) the performance of NeFL with ViTs in non-IID settings. We conduct experiments using the CIFAR-10 dataset [35] for image classification with ResNets. The experiments are evaluated with 5 submodels ( $N_s = 5$  where  $\gamma_1 = 0.2, \gamma_2 = 0.4, \gamma_3 = 0.6, \gamma_4 = 0.8, \gamma_5 = 1$ ) over a total 500 communication rounds ( $T$ ) with 100 clients ( $M$ ). At each round, a fraction rate of 0.1 is used, indicating that 10 clients ( $|C_t| = 10$ ) transmit their weights to the server. During the training process of clients, local batch size of 32 and a local epoch of  $E = 5$  are used. For training ResNets from scratch, we employ SGD optimizer [55] without momentum and weight decay. The initial learning rate is set to 0.1 and decreases by a factor of  $\frac{1}{10}$  at the halfway point and  $\frac{3}{4}$  of the total communication rounds. Pre-trained models we use for evaluation are trained on the ImageNet-1k dataset[14, 2]. To incorporate system heterogeneity, each client is assigned one of the submodels in each iteration and statistical heterogeneity was implemented by label distribution skew following Dirichlet distribution of concentration parameter 0.5 [66, 38].

As illustrated in Table 1, we observed that NeFL outperforms baselines for both the worst-case submodel ( $\gamma = 0.2$ ) and the average performance of the five submodels. We compared with other baselines by adjusting similar number of the parameters for each submodel. The details including computing costs (i.e., FLOPs) are described in the Appendix.



Table 3: Results of NeFL with three submodels for CIFAR-10 dataset under IID (left) and non-IID (right) settings. A initial weights for global model was given with the pre-trained model with ImageNet-1k. We report Top-1 classification accuracies (%) for the submodels.

Model	Param. #	Model size		Model	Param. #	Model size	
		Worst	Avg			Worst	Avg
ViT	86.4M	93.02	95.95	ViT	86.4M	87.56	93.50
Pre-trained Wide ResNet101 [67]	124.8M	90.9	91.35	Pre-trained Wide ResNet101 [67]	124.8M	87.17	87.74

We investigate the performance of incorporating pre-trained models into NeFL. Recent studies on FL figured out that FL gets benefits from pre-trained models even more than centralized learning [34, 9]. It motivates us to evaluate the performance of NeFL on pre-trained models. The pre-trained model that is trained in a common way with ImageNet-1k is loaded from PyTorch [52]. Even if pre-trained models are trained regardless of NeFL, the performance of NeFL was improved with pre-trained models. Furthermore, the results in Table 1 and Table 2 show that the performance of NeFL gets improved by pre-training for both IID and non-IID settings following the results of the recent studies. Meanwhile, baselines such as HeteroFL and DepthFL that do not have inconsistent parameters, when trained with pre-trained models, showed performance comparable to that of models trained from scratch.

We now present an experiment using ViTs and Wide ResNet [67]. The pre-trained weights trained on ImageNet-1k dataset [14] are loaded on the initial global models and subsequently NeFL was performed. The three submodels ( $N_s = 3$ ) of  $\gamma_1 = 0.5, \gamma_2 = 0.75, \gamma_3 = 1$  are given and the number of clients is  $M = 10$ , all of whom participate in the NeFL pipeline (with a fraction rate of 1). The experiment consists of  $T = 100$  communication rounds, and each client performs local training for a single epoch ( $E = 1$ ). We use a cosine annealing learning rate scheduling [46] with 500 steps of warmup and an initial learning rate 0.03. Note that utilizing layer normalization layers as consistent parameters, as opposed to BN layers that are inconsistent parameters, yields better performance.

Previous studies have examined the efficacy of ViTs in FL scenarios and found that ViTs can effectively alleviate the adverse effects of statistical heterogeneity due to their inherent robustness on distribution shifts [53]. Building upon this line of research, Table 3 demonstrates that ViTs outperform ResNets in both IID and non-IID settings, despite the larger number of parameters. Particularly in non-IID settings, ViTs exhibit significantly less performance degradation for average performance compared to IID setting across all model sizes.

## 6 Conclusion

In this work, we have introduced *Nested Federated Learning (NeFL)*, a generalized FL framework that addresses the challenges of system heterogeneity. By leveraging proposed depthwise and widthwise scaling, NeFL efficiently divides models into submodels employing the concept of ODE solver, leading to improved performance and enhanced compatibility with resource-constrained clients. We propose to decouple few parameters as inconsistent parameters for respective submodels that FedAvg are employed for averaging inconsistent parameters while NeFedAvg was utilized for averaging consistent parameters. Our experimental results highlight the significant performance gains achieved by NeFL, particularly for the worst-case submodel. Furthermore, we also explore NeFL in line with recent studies of FL such as pretraining and statistical heterogeneity.

## References

- [1] Data protection: Rules for the protection of personal data inside and outside the EU, 2022. [https://commission.europa.eu/law/law-topic/data-protection\\_en](https://commission.europa.eu/law/law-topic/data-protection_en) [Accessed: (2023/5/10)].
- [2] Pytorch models and pre-trained weights, 2023. <https://pytorch.org/vision/stable/models.html> [Accessed: (2023/5/16)].
- [3] Durmus Alp Emre Acar, Yue Zhao, Ramon Matas, Matthew Mattina, Paul Whatmough, and Venkatesh Saligrama. Federated learning based on dynamic regularization. In *International Conference on Learning Representations (ICLR)*, 2021.
- [4] Andrei Afonin and Sai Praneeth Karimireddy. Towards model agnostic federated learning using knowledge distillation. In *International Conference on Learning Representations (ICLR)*, 2022.
- [5] Manoj Ghuhan Arivazhagan, Vinay Aggarwal, Aaditya Kumar Singh, and Sunav Choudhary. Federated learning with personalization layers. *arXiv preprint arXiv:1912.00818*, 2019.
- [6] Thomas Bachlechner, Bodhisattwa Prasad Majumder, Henry Mao, Gary Cottrell, and Julian McAuley. Rezero is all you need: fast convergence at large depth. In *Conference on Uncertainty in Artificial Intelligence (UAI)*, 2021.
- [7] Cristian Buciluă, Rich Caruana, and Alexandru Niculescu-Mizil. Model compression. In *ACM SIGKDD International Conference on Knowledge Discovery and Data Mining (KDD)*, 2006.
- [8] Bo Chang, Lili Meng, Eldad Haber, Frederick Tung, and David Begert. Multi-level residual networks from dynamical systems view. In *International Conference on Learning Representations (ICLR)*, 2018.
- [9] Hong-You Chen, Cheng-Hao Tu, Ziwei Li, Han Wei Shen, and Wei-Lun Chao. On the importance and applicability of pre-training for federated learning. In *International Conference on Learning Representations (ICLR)*, 2023.
- [10] Ricky T. Q. Chen, Yulia Rubanova, Jesse Bettencourt, and David Duvenaud. Neural ordinary differential equations. In *Advances in Neural Information Processing Systems (NeurIPS)*, 2018.
- [11] Xiangning Chen, Cho-Jui Hsieh, and Boqing Gong. When vision transformers outperform resnets without pre-training or strong data augmentations. In *International Conference on Learning Representations (ICLR)*, 2022.
- [12] Ekin Dogus Cubuk, Barret Zoph, Jon Shlens, and Quoc Le. Randaugment: Practical automated data augmentation with a reduced search space. In *Advances in Neural Information Processing Systems (NeurIPS)*, 2020.
- [13] Luke N. Darlow, Elliot J. Crowley, Antreas Antoniou, and Amos J. Storkey. Cinic-10 is not imagenet or cifar-10. *arXiv preprint arXiv:1810.03505*, 2018.
- [14] Jia Deng, Wei Dong, Richard Socher, Li-Jia Li, Kai Li, and Li Fei-Fei. ImageNet: A large-scale hierarchical image database. In *IEEE/CVF Conference on Computer Vision and Pattern Recognition (CVPR)*, 2009.
- [15] Enmao Diao, Jie Ding, and Vahid Tarokh. HeteroFL: Computation and communication efficient federated learning for heterogeneous clients. In *International Conference on Learning Representations (ICLR)*, 2021.
- [16] Alexey Dosovitskiy, Lucas Beyer, Alexander Kolesnikov, Dirk Weissenborn, Xiaohua Zhai, Thomas Unterthiner, Mostafa Dehghani, Matthias Minderer, Georg Heigold, Sylvain Gelly, Jakob Uszkoreit, and Neil Houlsby. An image is worth 16x16 words: Transformers for image recognition at scale. In *International Conference on Learning Representations (ICLR)*, 2021.
- [17] Qi Dou, Tiffany Y So, Meirui Jiang, Quande Liu, Varut Vardhanabhuti, Georgios Kaissis, Zeju Li, Weixin Si, Heather HC Lee, Kevin Yu, et al. Federated deep learning for detecting COVID-19 lung abnormalities in CT: A privacy-preserving multinational validation study. *NPJ digital medicine*, 4(1):60, 2021.
- [18] Carl Eckart and Gale Young. The approximation of one matrix by another of lower rank. *Psychometrika*, 1(3):211–218, 1936.
- [19] David Ha, Andrew M. Dai, and Quoc V. Le. Hypernetworks. In *International Conference on Learning Representations (ICLR)*, 2017.
- [20] Farzin Haddadpour, Mohammad Mahdi Kamani, Aryan Mokhtari, and Mehrdad Mahdavi. Federated learning with compression: Unified analysis and sharp guarantees. In *International Conference on Artificial Intelligence and Statistics (AISTATS)*, 2021.

- [21] E. Hairer, S.P. Nørsett, and G. Wanner. *Solving Ordinary Differential Equations I Nonstiff problems*. Springer, Berlin, second edition, 2000.
- [22] Chaoyang He, Murali Annavam, and Salman Avestimehr. Group knowledge transfer: Federated learning of large cnns at the edge. In *Advances in Neural Information Processing Systems (NeurIPS)*, 2020.
- [23] Chaoyang He, Murali Annavam, and Salman Avestimehr. Group knowledge transfer: Federated learning of large cnns at the edge. In *Advances in Neural Information Processing Systems (NeurIPS)*, 2020.
- [24] Chaoyang He, Zhengyu Yang, Erum Mushtaq, Sunwoo Lee, Mahdi Soltanolkotabi, and Salman Avestimehr. SSFL: Tackling label deficiency in federated learning via personalized self-supervision. *arXiv preprint arXiv:2110.02470*, 2021.
- [25] Kaiming He, Xiangyu Zhang, Shaoqing Ren, and Jian Sun. Deep residual learning for image recognition. In *IEEE/CVF Conference on Computer Vision and Pattern Recognition (CVPR)*, 2016.
- [26] Yihui He, Xiangyu Zhang, and Jian Sun. Channel pruning for accelerating very deep neural networks. In *IEEE International Conference on Computer Vision (ICCV)*, 2017.
- [27] Geoffrey Hinton, Oriol Vinyals, and Jeff Dean. Distilling the knowledge in a neural network. *arXiv preprint arXiv:1503.02531*, 2015.
- [28] Junyuan Hong, Haotao Wang, Zhangyang Wang, and Jiayu Zhou. Efficient split-mix federated learning for on-demand and in-situ customization. In *International Conference on Learning Representations (ICLR)*, 2022.
- [29] Samuel Horváth, Stefanos Laskaridis, Mario Almeida, Ilias Leontiadis, Stylianos Venieris, and Nicholas Lane. FjORD: Fair and accurate federated learning under heterogeneous targets with ordered dropout. In *Advances in Neural Information Processing Systems (NeurIPS)*, 2021.
- [30] Gao Huang, Yu Sun, Zhuang Liu, Daniel Sedra, and Kilian Weinberger. Deep networks with stochastic depth. In *European Conference on Computer Vision (ECCV)*, 2016.
- [31] Yuang Jiang, Shiqiang Wang, Víctor Valls, Bong Jun Ko, Wei-Han Lee, Kin K. Leung, and Leandros Tassiulas. Model pruning enables efficient federated learning on edge devices. *IEEE Transactions on Neural Networks and Learning Systems (TNNLS)*, pages 1–13, 2022.
- [32] Peter Kairouz, H. Brendan McMahan, Brendan Avent, Aurélien Bellet, Mehdi Bennis, Arjun Nitin Bhagoji, Kallista Bonawit, Zachary Charles, Graham Cormode, Rachel Cummings, Rafael G. L. D’Oliveira, Hubert Eichner, Salim El Rouayheb, David Evans, Josh Gardner, Zachary Garrett, Adrià Gascón, Badi Ghazi, Phillip B. Gibbons, Marco Gruteser, Zaid Harchaoui, Chaoyang He, Lie He, Zhouyuan Huo, Ben Hutchinson, Justin Hsu, Martin Jaggi, Tara Javidi, Gauri Joshi, Mikhail Khodak, Jakub Konečný, Aleksandra Korolova, Farinaz Koushanfar, Sanmi Koyejo, Tancrède Lepoint, Yang Liu, Prateek Mittal, Mehryar Mohri, Richard Nock, Ayfer Özgür, Rasmus Pagh, Hang Qi, Daniel Ramage, Ramesh Raskar, Mariana Raykova, Dawn Song, Weikang Song, Sebastian U. Stich, Ziteng Sun, Ananda Theertha Suresh, Florian Tramèr, Praneeth Vepakomma, Jianyu Wang, Li Xiong, Zheng Xu, Qiang Yang, Felix X. Yu, Han Yu, and Sen Zhao. *Advances and Open Problems in Federated Learning*. Now Foundations and Trends, 2021.
- [33] Minjae Kim, Sangyoon Yu, Suhyun Kim, and Soo-Mook Moon. DepthFL : Depthwise federated learning for heterogeneous clients. In *International Conference on Learning Representations (ICLR)*, 2023.
- [34] Alexander Kolesnikov, Lucas Beyer, Xiaohua Zhai, Joan Puigcerver, Jessica Yung, Sylvain Gelly, and Neil Houlsby. Big transfer (BiT): General visual representation learning. In *European Conference on Computer Vision (ECCV)*, 2020.
- [35] Alex Krizhevsky, Vinod Nair, and Geoffrey Hinton. CIFAR-10 (Canadian Institute for Advanced Research). <http://www.cs.toronto.edu/~kriz/cifar.html>.
- [36] Namhoon Lee, Thalaiyasingam Ajanthan, Stephen Gould, and Philip HS Torr. A signal propagation perspective for pruning neural networks at initialization. In *International Conference on Learning Representations (ICLR)*, 2020.
- [37] Hao Li, Asim Kadav, Igor Durdanovic, Hanan Samet, and Hans Peter Graf. Pruning filters for efficient convnets. In *International Conference on Learning Representations (ICLR)*, 2017.
- [38] Qinbin Li, Yiqun Diao, Quan Chen, and Bingsheng He. Federated learning on non-iid data silos: An experimental study. *arXiv preprint arXiv:2102.02079*, 2021.

- [39] Qinbin Li, Bingsheng He, and Dawn Song. Model-contrastive federated learning. In *IEEE/CVF Conference on Computer Vision and Pattern Recognition*, 2021.
- [40] Tian Li, Anit Kumar Sahu, Ameet Talwalkar, and Virginia Smith. Federated learning: Challenges, methods, and future directions. *IEEE Signal Processing Magazine*, 37(3):50–60, May 2020.
- [41] Tian Li, Anit Kumar Sahu, Manzil Zaheer, Maziar Sanjabi, Ameet Talwalkar, and Virginia Smith. Federated optimization in heterogeneous networks. In *Machine Learning and Systems (MLSys)*, 2020.
- [42] Xiang Li, Kaixuan Huang, Wenhao Yang, Shusen Wang, and Zhihua Zhang. On the convergence of fedavg on non-iid data. In *International Conference on Learning Representations (ICLR)*, 2020.
- [43] Paul Pu Liang, Terrance Liu, Liu Ziyin, Ruslan Salakhutdinov, and Louis-Philippe Morency. Think locally, act globally: Federated learning with local and global representations. *arXiv preprint arXiv:2001.01523*, 2020.
- [44] Tao Lin, Lingjing Kong, Sebastian U Stich, and Martin Jaggi. Ensemble distillation for robust model fusion in federated learning. In *Advances in Neural Information Processing Systems (NeurIPS)*, 2020.
- [45] Zhuang Liu, Jianguo Li, Zhiqiang Shen, Gao Huang, Shoumeng Yan, and Changshui Zhang. Learning efficient convolutional networks through network slimming. In *IEEE International Conference on Computer Vision (ICCV)*, 2017.
- [46] Ilya Loshchilov and Frank Hutter. SGDR: Stochastic gradient descent with warm restarts. In *International Conference on Learning Representations (ICLR)*, 2017.
- [47] Ilya Loshchilov and Frank Hutter. Decoupled weight decay regularization. In *International Conference on Learning Representations (ICLR)*, 2019.
- [48] Disha Makhija, Nhat Ho, and Joydeep Ghosh. Federated self-supervised learning for heterogeneous clients. *arXiv preprint arXiv:2205.12493*, 2022.
- [49] Brendan McMahan, Eider Moore, Daniel Ramage, Seth Hampson, and Blaise Agüera y Arcas. Communication-efficient learning of deep networks from decentralized data. In *International Conference on Artificial Intelligence and Statistics (AISTATS)*, 2017.
- [50] Vaikkunth Mugunthan, Eric Lin, Vignesh Gokul, Christian Lau, Lalana Kagal, and Steve Pieper. FedLTN: Federated learning for sparse and personalized lottery ticket networks. In *European Conference on Computer Vision (ECCV)*, 2022.
- [51] Yuval Netzer, Tao Wang, Adam Coates, Alessandro Bissacco, Bo Wu, and Andrew Y. Ng. Reading digits in natural images with unsupervised feature learning. In *NIPS Workshop on Deep Learning and Unsupervised Feature Learning*, 2011.
- [52] Adam Paszke, Sam Gross, Francisco Massa, Adam Lerer, James Bradbury, Gregory Chanan, Trevor Killeen, Zeming Lin, Natalia Gimelshein, Luca Antiga, Alban Desmaison, Andreas Kopf, Edward Yang, Zachary DeVito, Martin Raison, Alykhan Tejani, Sasank Chilamkurthy, Benoit Steiner, Lu Fang, Junjie Bai, and Soumith Chintala. Pytorch: An imperative style, high-performance deep learning library. In *Advances in Neural Information Processing Systems (NeurIPS)*, 2019.
- [53] Liangqiong Qu, Yuyin Zhou, Paul Pu Liang, Yingda Xia, Feifei Wang, Ehsan Adeli, Li Fei-Fei, and Daniel Rubin. Rethinking architecture design for tackling data heterogeneity in federated learning. In *IEEE/CVF Conference on Computer Vision and Pattern Recognition (CVPR)*, 2022.
- [54] Daniel Rothchild, Ashwinee Panda, Enayat Ullah, Nikita Ivkin, Ion Stoica, Vladimir Braverman, Joseph Gonzalez, and Raman Arora. FetchSGD: Communication-efficient federated learning with sketching. In *International Conference on Machine Learning (ICML)*, 2020.
- [55] Sebastian Ruder. An overview of gradient descent optimization algorithms. *arXiv preprint arXiv:1609.04747*, 2016.
- [56] Shibani Santurkar, Dimitris Tsipras, Andrew Ilyas, and Aleksander Madry. How does batch normalization help optimization? In *Advances in Neural Information Processing Systems (NeurIPS)*, 2018.
- [57] Hyowoon Seo, Jihong Park, Seungeun Oh, Mehdi Bennis, and Seong-Lyun Kim. Federated knowledge distillation. *arXiv preprint arXiv:2011.02367*, 2020.

- [58] Christian Szegedy, Vincent Vanhoucke, Sergey Ioffe, Jon Shlens, and Zbigniew Wojna. Rethinking the inception architecture for computer vision. In *IEEE/CVF Conference on Computer Vision and Pattern Recognition (CVPR)*, pages 2818–2826, 2016.
- [59] Mingxing Tan and Quoc Le. EfficientNet: Rethinking model scaling for convolutional neural networks. In *International Conference on Machine Learning (ICML)*, 2019.
- [60] Chandra Thapa, Pathum Chamikara Mahawaga Arachchige, Seyit Camtepe, and Lichao Sun. Splitfed: When federated learning meets split learning. *AAAI Conference on Artificial Intelligence (AAAI)*, 2022.
- [61] Hugo Touvron, Matthieu Cord, Alexandre Sablayrolles, Gabriel Synnaeve, and Hervé Jégou. Going deeper with image transformers. In *IEEE International Conference on Computer Vision (ICCV)*, 2021.
- [62] Praneeth Vepakomma, Otkrist Gupta, Tristan Swedish, and Ramesh Raskar. Split learning for health: Distributed deep learning without sharing raw patient data. *arXiv preprint arXiv:1812.00564*, 2018.
- [63] Hongyi Wang, Mikhail Yurochkin, Yuekai Sun, Dimitris Papailiopoulos, and Yasaman Khazaeni. Federated learning with matched averaging. In *International Conference on Learning Representations (ICLR)*, 2020.
- [64] Chuhan Wu, Fangzhao Wu, Lingjuan Lyu, Yongfeng Huang, and Xing Xie. Communication-efficient federated learning via knowledge distillation. *Nature Communications*, 13(1), Apr. 2022.
- [65] Sangdoo Yun, Dongyoon Han, Seong Joon Oh, Sanghyuk Chun, Junsuk Choe, and Youngjoon Yoo. Cutmix: Regularization strategy to train strong classifiers with localizable features. In *IEEE International Conference on Computer Vision (ICCV)*, 2019.
- [66] Mikhail Yurochkin, Mayank Agarwal, Soumya Ghosh, Kristjan Greenewald, Nghia Hoang, and Yasaman Khazaeni. Bayesian nonparametric federated learning of neural networks. In *International Conference on Machine Learning (ICML)*, 2019.
- [67] Sergey Zagoruyko and Nikos Komodakis. Wide residual networks. In *British Machine Vision Conference (BMVC)*, 2016.
- [68] Hongyi Zhang, Moustapha Cisse, Yann N. Dauphin, and David Lopez-Paz. mixup: Beyond empirical risk minimization. In *International Conference on Learning Representations (ICLR)*, 2018.
- [69] Yue Zhao, Meng Li, Liangzhen Lai, Naveen Suda, Damon Civin, and Vikas Chandra. Federated learning with non-iid data. *arXiv preprint arXiv:1806.00582*, 2018.
- [70] Zhuangdi Zhu, Junyuan Hong, and Jiayu Zhou. Data-free knowledge distillation for heterogeneous federated learning. *arXiv preprint arXiv:2105.10056*, 2021.
- [71] Weiming Zhuang, Yonggang Wen, and Shuai Zhang. Divergence-aware federated self-supervised learning. In *International Conference on Learning Representations (ICLR)*, 2022.

# Supplementary Material

## A Additional Experiments

### A.1 Other Dataset

We evaluate the performance for other dataset such as CIFAR-100 [35], CINIC-10 [13] SVHN [51] dataset and we observe a similar trend to reported results in terms of Top-1 accuracy of the worst-case submodel and average accuracy over submodels. Note that we set total communication round  $T = 100$  for training SVHN. The results are presented in Table 4.

Table 4: Results of NeFL with five submodels for **CIFAR-100** (left), **CINIC10** (right) and **SVHN** (bottom) dataset under IID settings. We report Top-1 classification accuracies (%) for the worst-case submodel and the average of the performance of five submodels.

CIFAR-100				CINIC-10			
Model	Method	Model size		Model	Method	Model size	
		Worst	Avg			Worst	Avg
ResNet18	HeteroFL [15]	41.33	47.09	ResNet18	HeteroFL [15]	67.55	70.40
	FjORD [29]	49.29	52.67		FjORD [29]	71.95	74.98
	DepthFL [33]	31.68	49.56		DepthFL [33]	54.51	71.42
	<b>NeFL (ours)</b>	<b>52.63</b>	<b>53.62</b>		<b>NeFL (ours)</b>	<b>74.16</b>	<b>75.29</b>
ResNet34	HeteroFL [15]	34.96	39.75	ResNet34	HeteroFL [15]	67.39	69.62
	FjORD [29]	47.59	50.7		FjORD [29]	71.58	74.19
	DepthFL [33]	14.51	46.79		DepthFL [33]	32.05	67.04
	<b>NeFL (ours)</b>	<b>55.22</b>	<b>56.26</b>		<b>NeFL (ours)</b>	<b>75.02</b>	<b>76.68</b>

SVHN			
Model	Method	Model size	
		Worst	Avg
ResNet18	HeteroFL [15]	91.82	93.46
	FjORD [29]	94.31	93.97
	DepthFL [33]	91.54	93.97
	<b>NeFL (ours)</b>	<b>94.45</b>	<b>94.94</b>
ResNet34	HeteroFL [15]	89.86	92.39
	FjORD [29]	93.83	94.63
	DepthFL [33]	74.33	89.96
	<b>NeFL (ours)</b>	<b>94.72</b>	<b>95.22</b>

### A.2 Different Number of Clients

We conducted further experiments on various numbers of clients while keeping the total amount of dataset. In Table 5, We could observe that as the number of clients increases, the performance of NeFL as well as baselines degrades. The results align with previous studies [33, 60, 63]. The more the number of clients, training data deviates further from being IID. While the IID sampling of the training data ensures the stochastic gradient to be an unbiased estimate of the full gradient, the non-IID sampling leads to non-guaranteed convergence and model weight divergence in FL [41, 39, 69]. In this regard, our proposed algorithm remains effective across different numbers of clients; however, the performance (e.g., accuracy and convergence) degrades due to changes in data distribution among clients as their number increases.

Table 5: Results of NeFL of five submodels with a global model ResNet18 for CIFAR-10 dataset under IID settings across different number of clients. We report Top-1 classification accuracies (%) for the worst-case submodel and the average of the performance of five submodels..

# of Clients	Model size	Method			
		NeFL (ours)	FjORD [29]	HeteroFL [15]	DepthFL [33]
100	Worst	<b>86.86</b>	85.12	80.62	64.8
	Avg	<b>87.88</b>	87.32	84.62	82.44
50	Worst	<b>88.42</b>	86.19	84.67	52.07
	Avg	<b>89.14</b>	88.43	87.23	82.04
20	Worst	<b>89.2</b>	87.76	88.74	24.94
	Avg	<b>89.88</b>	89.6	88.71	76.54

### A.3 Ablation Study

For the ease of understanding for ablation study we refer *NeFL-W* that all submodels are scaled widthwise, *NeFL-D* that all submodels are scaled depthwise and *NeFL-WD* that submodels are scaled both widthwise and depthwise. We further refer to NeFL-D<sub>O</sub> that has different initial step sizes with NeFL-D. Referring to Table 12, NeFL-D<sub>O</sub> has larger magnitude step sizes compared to NeFL-D<sub>D</sub>, aligning with the principles of ODE solver. NeFL-D<sub>D</sub> scales submodels by skipping a subset of blocks of a global model, thus reducing the depth of the model. NeFL-D<sub>D</sub> does not compensate for the skipped blocks by using larger step sizes. Given the initial step sizes as  $s_0 = 1, s_1 = 1, s_2 = 0$ , output after Block 2 without Block 2 is  $\mathbf{Y}_3 = \mathbf{Y}_0 + F_0 + F_1$ . NeFL-D<sub>O</sub> reduces the size of the global model by skipping a subset of block functions  $F(\cdot)$  and gives larger initial step sizes to compensate it. The step sizes are determined based on the number of blocks that are skipped. A model without Block 2, output after Block 2 is initially computed as  $\mathbf{Y}_3 = \mathbf{Y}_0 + F_0 + 2F_1$ .

The performance comparison between NeFL-W and FjORD [29] provides the effectiveness of learnable step sizes and comparison between NeFL-W and HeteroFL [15] provides the effectiveness of inconsistent parameters including learnable step sizes. Similarly, the comparison between NeFL-D and NeFL-D with no learnable step sizes (N/L; constant step sizes with given initial values) provides the effectiveness of learnables step sizes and comparison between NeFL-D and DepthFL [33] (NeFL-WD and NeFL-WD (N/L)) provides the effectiveness of inconsistent parameters. We summarized the NeFL with various scaled submodels in Table 7. We also provide the parameter sizes and average FLOPs of submodels by scaling in Table 8.

Insights can be derived from the ablation studies (Table 6) conducted on the NeFL framework. We observe that NeFL-D outperforms NeFL-D<sub>O</sub> in most cases. The rationale comes from the trained step sizes are not as large as initial value for NeFL-D<sub>O</sub> that large values for NeFL-D<sub>O</sub> degrades the trainability of depthwise-scaled submodels. The performance improvement of NeFL-WD over NeFL-WD, NeFL-D over NeFL-D (N/L) and NeFL-W over FjORD [29] provides the effectiveness of learnable step sizes. The effectiveness of the proposed parameter averaging for consistent parameters and inconsistent parameters is also verified by NeFL-D over DepthFL [33] and NeFL-W over HeteroFL [15]. Furthermore, We observe that NeFL-D and NeFL-WD have better performance over widthwise scaling. The performance gap of depthwise scaling over widthwise scaling gets larger for narrow and deeper networks.

We evaluated the experiments by similar number of parameters for several scaling methods and depthwise scaling requires slightly more FLOPs than widthwise scaling for ResNet18, ResNet34 and ResNet110 and less FLOPs for ResNet56. Note that beyond the performance improvement, NeFL provides the more degree-of-freedom for widthwise/depthwise scaling that can be determined by the requirements of clients while NeFL-W also outperforms baselines in Table 6. Also refer to Table 9 that has different scaling ratio. Note that in this case, FjORD [29] outperforms NeFL-W. In this case with severe scaling factors (the worst model has 4% parameters of a global model), step sizes could not compensate the limited number of parameters and degraded the trainability with auxiliary parameters.

Table 6: Ablation study by NeFL with five submodels for CIFAR-10 dataset under IID settings. We report Top-1 classification accuracies (%) for the worst-case submodel and the average of the performance of five submodels.

Model	Method	Model size	
		Worst	Avg
ResNet18	HeteroFL [15]	80.62	84.26
	FjORD [29]	85.12	87.32
	<b>NeFL-W</b>	<b>85.13</b>	<b>87.36</b>
	DepthFL [33]	64.80	82.44
	NeFL-D (N/L)	86.29	88.12
	NeFL-D <sub>O</sub> (N/L)	86.24	88.22
	<b>NeFL-D</b>	<b>86.06</b>	<b>87.94</b>
	NeFL-D <sub>O</sub>	85.98	88.20
	<b>NeFL-WD</b>	<b>86.86</b>	<b>87.88</b>
	NeFL-WD (N/L)	86.85	88.21
Model	Method	Model size	
		Worst	Avg
ResNet34	HeteroFL [15]	79.51	83.16
	FjORD [29]	85.12	87.36
	<b>NeFL-W</b>	<b>85.65</b>	<b>87.97</b>
	DepthFL [33]	25.73	75.30
	NeFL-D (N/L)	87.40	89.12
	NeFL-D <sub>O</sub> (N/L)	86.47	88.49
	<b>NeFL-D</b>	<b>87.71</b>	<b>89.02</b>
	NeFL-D <sub>O</sub>	87.06	88.71
	<b>NeFL-WD</b>	<b>86.73</b>	<b>88.42</b>
	NeFL-WD (N/L)	86.2	88.16
Model	Method	Model size	
		Worst	Avg
Pre-trained ResNet18	HeteroFL [15]	78.26	84.06
	FjORD [29]	86.37	88.91
	<b>NeFL-W</b>	<b>86.1</b>	<b>89.13</b>
	DepthFL [33]	47.76	82.85
	NeFL-D (N/L)	86.95	89.77
	NeFL-D <sub>O</sub> (N/L)	86.24	89.76
	<b>NeFL-D</b>	<b>87.13</b>	<b>90.00</b>
	NeFL-D <sub>O</sub>	87.02	89.72
	<b>NeFL-WD</b>	<b>88.61</b>	<b>89.60</b>
	NeFL-WD (N/L)	88.57	89.70
Model	Method	Model size	
		Worst	Avg
Pre-trained ResNet34	HeteroFL [15]	79.97	84.34
	FjORD [29]	87.08	89.37
	<b>NeFL-W</b>	<b>87.41</b>	<b>89.75</b>
	DepthFL [33]	52.08	83.63
	NeFL-D (N/L)	87.95	90.79
	NeFL-D <sub>O</sub> (N/L)	87.44	90.58
	<b>NeFL-D</b>	<b>88.36</b>	<b>91.14</b>
	NeFL-D <sub>O</sub>	87.86	90.90
	<b>NeFL-WD</b>	<b>87.69</b>	<b>90.18</b>
	NeFL-WD (N/L)	87.37	89.78
Model	Method	Model size	
		Worst	Avg
ResNet56	HeteroFL [15]	65.09	74.13
	FjORD [29]	81.38	84.77
	<b>NeFL-W</b>	<b>82.05</b>	<b>85.48</b>
	DepthFL [33]	72.94	86.19
	NeFL-D (N/L)	84.38	86.13
	NeFL-D <sub>O</sub> (N/L)	83.08	85.59
	<b>NeFL-D</b>	<b>84.38</b>	<b>86.13</b>
	NeFL-D <sub>O</sub>	81.97	85.37
	<b>NeFL-WD</b>	<b>83.92</b>	<b>86.00</b>
	NeFL-WD (N/L)	83.68	85.85
Model	Method	Model size	
		Worst	Avg
ResNet110	HeteroFL [15]	54.83	67.33
	FjORD [29]	81.70	85.16
	<b>NeFL-W</b>	<b>81.67</b>	<b>85.32</b>
	DepthFL [33]	73.56	82.42
	NeFL-D (N/L)	85.23	86.34
	NeFL-D <sub>O</sub> (N/L)	84	85.97
	<b>NeFL-D</b>	<b>85.96</b>	<b>86.66</b>
	NeFL-D <sub>O</sub>	82.74	85.66
	<b>NeFL-WD</b>	<b>84.41</b>	<b>86.28</b>
	NeFL-WD (N/L)	83.58	85.73



Table 7: Summarization of NeFL and baselines for ablation study

	Depthwise scaling	Widthwise scaling	Adaptive step sizes
DepthFL	✓		
FjORD, HeteroFL		✓	
NeFL-D	✓		✓
NeFL-W		✓	✓
NeFL-WD	✓	✓	✓

Table 8: Details of average FLOPs of submodels of  $\gamma = [0.2, 0.4, 0.6, 0.8, 1]$ 

Model	Metric	Method		
		Width/Depthwise scaling	Widthwise scaling	Depthwise scaling
ResNet18	Param #	6.71M	6.71M	6.68M
	FLOPs	87.8M	85M	102M
ResNet34	Param #	12.6M	12.8M	12.9M
	FLOPs	181M	176M	193M
ResNet56	Param #	0.51M	0.52M	0.51M
	FLOPs	530M	534M	526M
ResNet110	Param #	1.05M	1.06M	1.04M
	FLOPs	158M	159M	234M

Table 9: Results of NeFL with five submodels ( $\gamma = [0.04, 0.16, 0.36, 0.64, 1]$ ) for CIFAR-10 dataset on ResNet110. Results of NeFL with five submodels for CIFAR-10 dataset under IID settings. We report Top-1 classification accuracies (%) for the worst-case submodel and the average of the performance of five submodels.

Model	Method	Model size	
		Worst	Avg
ResNet110	HeteroFL [15]	46.58	63.62
	FjORD [29]	69.61	81.46
	<b>NeFL-W</b>	68.27	80.98
	DepthFL [33]	11.00	53.91
	<b>NeFL-D</b>	<b>75.4</b>	<b>84.31</b>
	<b>NeFL-WD</b>	<b>76.60</b>	<b>84.02</b>

## B Experimental Details

### B.1 Model Architectures

For the experiments presented in Table 1, Table 2, Table 4, Table 5 and Table 6, we consider five submodels with  $\gamma = [\gamma_1, \gamma_2, \gamma_3, \gamma_4, \gamma_5] = [0.2, 0.4, 0.6, 0.8, 1]$  and  $\gamma = [0.04, 0.16, 0.36, 0.64, 1]$  for Table 9. Additionally, for Table 3, we use three submodels with  $\gamma = [\gamma_1, \gamma_2, \gamma_3] = [0.5, 0.75, 1]$ .

The ResNet18 architecture (detailed in Table 10) and ResNet34 architecture (detailed in Table 11) consist of four layers, while ResNet56 (detailed in Table 12) and ResNet110 (detailed in Table 14) have three layers. These layers are composed of blocks with different channel sizes, specifically (64, 128, 256, 512) for ResNet18/32 and (16, 32, 64) for ResNet56/110. Wide ResNet101\_2 (detailed in Table 15) comprises four layers of bottleneck blocks with channel sizes (128, 256, 512, 1024) [25, 67]. The ViT-B/16 architecture consists of twelve layers, with each layer containing blocks comprising self-attention (SA) and feed-forward networks (FFN) [16]. The widthwise splitting for ViT models are implemented by varying the embedding dimension ( $D$  in [16]). In the tables, 1's and 0's denote the step sizes. A step size of zero indicates that a submodel does not include the corresponding block. Unlike ResNets, which have a step size for each block, ViTs have different learnable step size parameters to be multiplied with SA and FFN. NeFL-W is characterized by  $\gamma_D = [1, \dots, 1]$  and  $\gamma_W$  with a target size, NeFL-D is characterized by  $\gamma_W = [1, \dots, 1]$  and  $\gamma_D$  with a target size and NeFL-WD is characterized by target size  $\gamma_W \gamma_D$ . NeFL on Table 1 and Table 2 follows NeFL-WD (for ResNet18 and ResNet110) and NeFL-DD (for ResNet 34 and ResNet 56). Corresponding number of parameters and FLOPs is provided in Table 8.

### B.2 Dataset

**CIFAR10/100** The CIFAR10 dataset consists of 60000 images (train dataset consists of 50000 samples and test dataset consists of 10000 samples).  $32 \times 32 \times 3$  color images are categorized by 10 classes, with 6000 images per class [35]. For FL with each client has 500 data samples for  $M = 100$ , and 5000 data samples for  $M = 10$ . We perform data augmentation and pre-processing of random cropping (by  $32 \times 32$  with padding of 4), random horizontal flip, and normalization by mean of (0.4914, 0.4822, 0.4465) and standard deviation of (0.2023, 0.1994, 0.2010).

**CINIC10** The CIFAR10 dataset consists of 270000  $32 \times 32 \times 3$  color images (train dataset consists of 90000 samples and validation and test dataset consists of 90000 samples respectively) in 10 classes [13]. It is constructed from ImageNet and CIFAR10. We perform data augmentation and pre-processing of random cropping (by  $32 \times 32$  with padding of 4), random horizontal flip, and normalization by mean of (0.47889522, 0.47227842, 0.43047404) and standard deviation of (0.24205776, 0.23828046, 0.25874835).

**SVHN** The SVHN dataset consists of 73257 digits for training and 26032 digits for testing of  $32 \times 32 \times 3$  color images [51]. The dataset is obtained from house numbers in Google Street view images in 10 classes (digit '0' to digit '9'). For FL for  $M = 100$  each client has 732 samples. We perform data augmentation and pre-processing of random cropping (by  $32 \times 32$  with padding of 2), color jitter (by brightness of 63/255, saturation=[0.5, 1.5] and contrast=[0.2, 1.8] implemented by `torchvision.transforms.ColorJitter`), and normalization by mean of (0.4376821, 0.4437697, 0.47280442) and standard deviation of (0.19803012, 0.20101562, 0.19703614).

### B.3 Baselines

**DepthFL[33]** The model is split depthwise, and an auxiliary bottleneck layer is included as an independent classifier. We implement DepthFL without separate bottleneck layers to be a special case of NeFL-DD with contiguous skipping blocks. In this special case, each submodels is a subset of the larger submodels. Our DepthFL models incorporate downsampling layers that adjust the feature size to match the input sizes of the classifier. It is important to note that the auxiliary bottleneck layers for submodels in DepthFL can be interpreted as parameter decoupling, as discussed in Section 4.2. Furthermore, we enhance DepthFL also by incorporating our proposed parameter decoupling techniques (i.e., BN layers decoupling). This addresses the issue of inconsistency and further improves the performance of DepthFL.

**HeteroFL & FjORD [15, 29]** HeteroFL [15] and FjORD [29] are two widthwise splitting methods designed to address the challenges posed by client heterogeneity in FL. While both methods aim to mitigate the impact of heterogeneity, these are several key differences between them. Firstly, HeteroFL does not utilize separate (i.e., inconsistent) parameters for BN layers in its submodels, whereas FjORD incorporates distinct BN layer for each submodel. This difference in handling BN layers can impact the learning dynamics and model performance. Secondly, HeteroFL employs static batch normalization, where BN statistics are updated using the entire dataset after the training process. On the other hand, FjORD updates BN statistics during training. Lastly, HeteroFL utilizes a masked cross-entropy loss to address the statistical heterogeneity among clients. This loss function helps to mitigate the impact of clients with the statistical heterogeneity. However, in our implementation of HeteroFL, the masked cross-entropy loss is not utilized.

#### B.4 Pre-trained models

The pre-trained models on Table 3 and Table 2 are trained on ImageNet-1k [14] as following recipes [2]:

**ResNet18/34** The models are trained by epochs of 90, batch size of 32, SGD optimizer [55], learning rate of 0.1 with momentum of 0.9 and weight decay of 0.0001, where learning rate is decreased by a factor of 0.1 every 30 epochs.

**Wide ResNet101\_2** The model is trained by epochs of 90, batch size of 32, SGD optimizer [55], learning rate of 0.1 with momentum of 0.9 and weight decay of 0.0001, where the learning scheduler is cosine learning rate [46] and warming up restarts for 256 epochs.

**ViT-B/16** The model is trained by epochs of 300, batch size of 512, AdamW optimizer [47] with learning rate of 0.003 and weight decay of 0.3. The learning scheduler is cosine annealing [46] after linear warmup method with decay of 0.033 for 30 epochs. Additionally, the random augmentation [12], random mixup with  $\alpha = 0.2$  [68], cutmix of  $\alpha = 1$  [65], repeated augmentation, label smoothing of 0.11 [58], clipping gradient norm to 1, model exponential moving average (EMA) are employed.

#### B.5 Dynamic environment

We simulate a dynamic environment by randomly selecting which model to train for each client during every communication round. In our experiments for Table 1 and Table ??, we have an equal number of five tiers of clients ( $M/N_s = 20$  for all tiers of clients). The resource-constrained clients (tier 1) randomly select models between  $\gamma = 0.2, 0.4, 0.6$ , clients in tier 2 randomly select models from the set  $\gamma = 0.2, 0.4, 0.6, 0.8$ , clients in tier 3 randomly select models from the set  $\gamma = 0.2, 0.4, 0.6, 0.8, 1$ , clients in tier 4 randomly select models from the set  $\gamma = 0.4, 0.6, 0.8, 1$ , and the resource-richest clients (tier 5) randomly select models from the set  $\gamma = 0.6, 0.8, 1$ . In our experiments for Table ?? involving three submodels and 10 clients, the tier 1 clients (3 out of 10 total clients) select  $\gamma = 0.5$ , tier 2 clients (3 out of 10 total clients) select  $\gamma = 0.75$  and tier 3 clients (4 out of 10 total clients) select  $\gamma = 1$ . By allowing clients to randomly choose from the available submodels, our setup reflects the dynamic nature in which clients may encounter communication computing bottlenecks during each iteration.

Table 10: Details of  $\gamma$  of NeFL on ResNet18

Model size			NeFL-D (ResNet18)			
$\gamma$	$\gamma_W$	$\gamma_D$	Layer 1 (64)	Layer 2 (128)	Layer3 (256)	Layer 4 (512)
0.2	1	0.20	1,1	0,0	1,1	0,0
0.4	1	0.38	1,0	0,0	1,0	1,0
0.6	1	0.57	1,1	1,1	1,1	1,0
0.8	1	0.81	1,0	1,1	0,0	1,1
1	1	1	1,1	1,1	1,1	1,1

Model size			NeFL-WD (ResNet18)			
$\gamma$	$\gamma_W$	$\gamma_D$	Layer 1 (64)	Layer 2 (128)	Layer3 (256)	Layer 4 (512)
0.2	0.34	0.58	1,1	1,1	1,1	1,0
0.4	0.4	1	1,1	1,1	1,1	1,1
0.6	0.6	1	1,1	1,1	1,1	1,1
0.8	0.8	1	1,1	1,1	1,1	1,1
1	1	1	1,1	1,1	1,1	1,1

Table 11: Details of  $\gamma$  of NeFL on ResNet34

Model size			NeFL-D (ResNet34)			
$\gamma$	$\gamma_W$	$\gamma_D$	Layer 1 (64)	Layer 2 (128)	Layer3 (256)	Layer 4 (512)
0.2	1	0.23	1,0,0	1,0,0,0	1,0,0,0,0	1,0,0
0.4	1	0.39	1,1,1	1,1,1,1	1,1,0,0,1	1,0,0
0.6	1	0.61	1,1,1	1,1,1,1	1,1,0,0,1	1,0,1
0.8	1	0.81	1,1,1	1,0,0,1	1,1,0,0,1	1,1,1
1	1	1	1,1,1	1,1,1,1	1,1,1,1,1	1,1,1

Model size			NeFL-WD (ResNet34)			
$\gamma$	$\gamma_W$	$\gamma_D$	Layer 1 (64)	Layer 2 (128)	Layer3 (256)	Layer 4 (512)
0.2	0.38	0.53	1,1,1	1,0,0,1	1,0,0,0,1	1,0,1
0.4	0.63	0.64	1,1,1	1,0,0,1	1,1,1,0,0,1	1,0,1
0.6	0.77	0.78	1,1,1	1,1,1,1	1,1,1,1,0,1	1,0,1
0.8	0.90	0.89	1,1,1	1,1,1,1	1,1,1,0,0,1	1,1,1
1	1	1	1,1,1	1,1,1,1	1,1,1,1,1,1	1,1,1

Table 12: Details of  $\gamma$  of NeFL on ResNet56

Model size			NeFL-D (ResNet56)		
$\gamma$	$\gamma_W$	$\gamma_D$	Layer 1 (16)	Layer 2 (32)	Layer3 (64)
0.2	1	0.2	1,1,0,0,0,0,0,0,0,0	1,1,0,0,0,0,0,0,0,0	1,1,0,0,0,0,0,0,0,0
0.4	1	0.4	1,1,1,0,0,0,0,0,0,0	1,1,1,0,0,0,0,0,0,0	1,1,1,1,0,0,0,0,0,0
0.6	1	0.6	1,1,1,1,0,0,0,0,0,0	1,1,1,1,0,0,0,0,0,0	1,1,1,1,1,1,0,0,0,0
0.8	1	0.8	1,1,1,1,1,1,1,1,1,1	1,1,1,1,1,1,1,1,1,0	1,1,1,1,1,1,1,1,0,0
1	1	1	1,1,1,1,1,1,1,1,1,1	1,1,1,1,1,1,1,1,1,1	1,1,1,1,1,1,1,1,1,1

Model size			NeFL-D <sub>O</sub> (ResNet56)		
$\gamma$	$\gamma_W$	$\gamma_D$	Layer 1 (16)	Layer 2 (32)	Layer3 (64)
0.2	1	0.2	1,8,0,0,0,0,0,0,0,0	1,8,0,0,0,0,0,0,0,0	1,8,0,0,0,0,0,0,0,0
0.4	1	0.4	1,1,7,0,0,0,0,0,0,0	1,1,7,0,0,0,0,0,0,0	1,1,1,6,0,0,0,0,0,0
0.6	1	0.6	1,1,1,6,0,0,0,0,0,0	1,1,1,6,0,0,0,0,0,0	1,1,1,1,4,0,0,0,0,0
0.8	1	0.8	1,1,1,1,1,1,1,1,1,1	1,1,1,1,1,1,1,1,2,0	1,1,1,1,1,1,3,0,0,0
1	1	1	1,1,1,1,1,1,1,1,1,1	1,1,1,1,1,1,1,1,1,1	1,1,1,1,1,1,1,1,1,1

Model size			NeFL-WD (ResNet56)		
$\gamma$	$\gamma_W$	$\gamma_D$	Layer 1 (16)	Layer 2 (32)	Layer3 (64)
0.2	0.46	0.43	1,1,1,1,0,0,0,0,0,0	1,1,1,1,0,0,0,0,0,0	1,1,1,1,0,0,0,0,0,0
0.4	0.61	0.66	1,1,1,1,1,1,0,0,0,0	1,1,1,1,1,1,0,0,0,0	1,1,1,1,1,1,0,0,0,0
0.6	0.77	0.77	1,1,1,1,1,1,1,0,0,0	1,1,1,1,1,1,1,0,0,0	1,1,1,1,1,1,1,0,0,0
0.8	0.90	89	1,1,1,1,1,1,1,1,0,0	1,1,1,1,1,1,1,1,0,0	1,1,1,1,1,1,1,1,0,0
1	1	1	1,1,1,1,1,1,1,1,1,1	1,1,1,1,1,1,1,1,1,1	1,1,1,1,1,1,1,1,1,1

Table 13: Details of  $\gamma$  of NeFL on ViT-B/16

Model size			NeFL-D (ViT-B/16)	Model size			NeFL-W (ViT-B/16)
$\gamma$	$\gamma_W$	$\gamma_D$	Block	$\gamma$	$\gamma_W$	$\gamma_D$	Block
0.5	1	0.50	1,1,1,1,1,1,0,0,0,0,0,0	0.5	0.5	1	1,1,1,1,1,1,1,1,1,1,1,1
0.75	1	0.75	1,1,1,1,1,1,1,1,0,0,0,0	0.75	0.75	1	1,1,1,1,1,1,1,1,1,1,1,1
1	1	1	1,1,1,1,1,1,1,1,1,1,1,1	1	1	1	1,1,1,1,1,1,1,1,1,1,1,1

Table 14: Details of  $\gamma$  of NeFL on ResNet110

Model size		NeFL-D (ResNet110)			
$\gamma$	$\gamma_W$	$\gamma_D$	Layer 1 (16)	Layer 2 (32)	Layer3 (64)
0.2	1	0.20	1, 1, 1, 1, 1, 1, 1, 1, 1, 1, 1, 1, 1, 1, 1, 1, 0, 0	1, 1, 1, 1, 0, 0, 0, 0, 0, 0, 0, 0, 0, 0, 0, 0, 0, 0	1, 1, 1, 0, 0, 0, 0, 0, 0, 0, 0, 0, 0, 0, 0, 0, 0, 0
0.4	1	0.40	1, 1, 1, 1, 1, 1, 1, 1, 1, 1, 1, 1, 1, 1, 1, 1, 0, 0, 0, 0	1, 1, 1, 1, 1, 1, 1, 0, 0, 0, 0, 0, 0, 0, 0, 0, 0, 0, 0	1, 1, 1, 1, 1, 1, 1, 1, 0, 0, 0, 0, 0, 0, 0, 0, 0, 0
0.6	1	0.60	1, 1, 1, 1, 1, 1, 1, 1, 1, 1, 1, 1, 1, 1, 1, 1, 0, 0	1, 1, 1, 1, 1, 1, 1, 1, 1, 1, 1, 1, 1, 1, 0, 0, 0, 0	1, 1, 1, 1, 1, 1, 1, 1, 1, 1, 0, 0, 0, 0, 0, 0, 0, 0
0.8	1	0.80	1, 1, 1, 1, 1, 1, 1, 1, 1, 1, 1, 1, 1, 1, 1, 1, 0, 0	1, 1, 1, 1, 1, 1, 1, 1, 1, 1, 1, 1, 1, 1, 1, 1, 0, 0	1, 1, 1, 1, 1, 1, 1, 1, 1, 1, 1, 1, 1, 1, 1, 1, 0, 0, 0
1	1	1	1, 1, 1, 1, 1, 1, 1, 1, 1, 1, 1, 1, 1, 1, 1, 1, 1, 1	1, 1, 1, 1, 1, 1, 1, 1, 1, 1, 1, 1, 1, 1, 1, 1, 1, 1	1, 1, 1, 1, 1, 1, 1, 1, 1, 1, 1, 1, 1, 1, 1, 1, 1, 1, 1
Model size		NeFL-WD (ResNet110)			
$\gamma$	$\gamma_W$	$\gamma_D$	Layer 1 (16)	Layer 2 (32)	Layer3 (64)
0.2	0.46	0.44	1, 1, 1, 1, 1, 1, 1, 1, 0, 0, 0, 0, 0, 0, 0, 0, 0, 1	1, 1, 1, 1, 1, 1, 1, 0, 0, 0, 0, 0, 0, 0, 0, 0, 0, 1	1, 1, 1, 1, 1, 1, 1, 1, 0, 0, 0, 0, 0, 0, 0, 0, 0, 1
0.4	0.60	0.66	1, 1, 1, 1, 1, 1, 1, 1, 1, 1, 1, 0, 0, 0, 0, 0, 0, 1	1, 1, 1, 1, 1, 1, 1, 1, 1, 1, 0, 0, 0, 0, 0, 0, 0, 1	1, 1, 1, 1, 1, 1, 1, 1, 1, 1, 1, 1, 1, 1, 0, 0, 0, 0, 1
0.6	0.77	0.77	1, 1, 1, 1, 1, 1, 1, 1, 1, 1, 1, 1, 0, 0, 0, 0, 0, 1	1, 1, 1, 1, 1, 1, 1, 1, 1, 1, 1, 1, 1, 0, 0, 0, 0, 1	1, 1, 1, 1, 1, 1, 1, 1, 1, 1, 1, 1, 1, 1, 1, 0, 0, 0, 1
0.8	0.90	0.89	1, 1, 1, 1, 1, 1, 1, 1, 1, 1, 1, 1, 1, 1, 0, 0, 0, 1	1, 1, 1, 1, 1, 1, 1, 1, 1, 1, 1, 1, 1, 1, 1, 0, 0, 1	1, 1, 1, 1, 1, 1, 1, 1, 1, 1, 1, 1, 1, 1, 1, 1, 0, 0, 1
1	1	1	1, 1, 1, 1, 1, 1, 1, 1, 1, 1, 1, 1, 1, 1, 1, 1, 1, 1	1, 1, 1, 1, 1, 1, 1, 1, 1, 1, 1, 1, 1, 1, 1, 1, 1, 1	1, 1, 1, 1, 1, 1, 1, 1, 1, 1, 1, 1, 1, 1, 1, 1, 1, 1, 1
Model size		NeFL-D (ResNet110)			
$\gamma$	$\gamma_W$	$\gamma_D$	Layer 1 (16)	Layer 2 (32)	Layer3 (64)
0.04	1	0.04	1, 0, 0, 0, 0, 0, 0, 0, 0, 0, 0, 0, 0, 0, 0, 0, 0, 0	1, 0, 0, 0, 0, 0, 0, 0, 0, 0, 0, 0, 0, 0, 0, 0, 0, 0	1, 0, 0, 0, 0, 0, 0, 0, 0, 0, 0, 0, 0, 0, 0, 0, 0, 0
0.16	1	0.16	1, 1, 1, 1, 0, 0, 0, 0, 0, 0, 0, 0, 0, 0, 0, 0, 0, 0	1, 1, 1, 0, 0, 0, 0, 0, 0, 0, 0, 0, 0, 0, 0, 0, 0, 0	1, 1, 1, 0, 0, 0, 0, 0, 0, 0, 0, 0, 0, 0, 0, 0, 0, 0
0.36	1	0.37	1, 1, 1, 1, 1, 0, 0, 0, 0, 0, 0, 0, 0, 0, 0, 0, 0, 0	1, 1, 1, 1, 1, 0, 0, 0, 0, 0, 0, 0, 0, 0, 0, 0, 0, 0	1, 1, 1, 1, 1, 1, 0, 0, 0, 0, 0, 0, 0, 0, 0, 0, 0, 0
0.64	1	0.65	1, 1, 1, 1, 1, 1, 1, 1, 0, 0, 0, 0, 0, 0, 0, 0, 0, 0	1, 1, 1, 1, 1, 1, 1, 1, 1, 0, 0, 0, 0, 0, 0, 0, 0	1, 1, 1, 1, 1, 1, 1, 1, 1, 1, 1, 1, 1, 1, 0, 0, 0, 0
1	1	1	1, 1, 1, 1, 1, 1, 1, 1, 1, 1, 1, 1, 1, 1, 1, 1, 1, 1	1, 1, 1, 1, 1, 1, 1, 1, 1, 1, 1, 1, 1, 1, 1, 1, 1, 1	1, 1, 1, 1, 1, 1, 1, 1, 1, 1, 1, 1, 1, 1, 1, 1, 1, 1
Model size		NeFL-WD (ResNet110)			
$\gamma$	$\gamma_W$	$\gamma_D$	Layer 1 (16)	Layer 2 (32)	Layer3 (64)
0.04	0.26	0.16	1, 1, 1, 0, 0, 0, 0, 0, 0, 0, 0, 0, 0, 0, 0, 0, 0, 0	1, 1, 1, 0, 0, 0, 0, 0, 0, 0, 0, 0, 0, 0, 0, 0, 0, 0	1, 1, 1, 0, 0, 0, 0, 0, 0, 0, 0, 0, 0, 0, 0, 0, 0, 0
0.16	0.42	0.38	1, 1, 1, 1, 1, 1, 0, 0, 0, 0, 0, 0, 0, 0, 0, 0, 0, 0	1, 1, 1, 1, 1, 1, 0, 0, 0, 0, 0, 0, 0, 0, 0, 0, 0, 0	1, 1, 1, 1, 1, 1, 1, 0, 0, 0, 0, 0, 0, 0, 0, 0, 0
0.36	0.59	0.61	1, 1, 1, 1, 1, 1, 1, 1, 1, 0, 0, 0, 0, 0, 0, 0, 0, 0	1, 1, 1, 1, 1, 1, 1, 1, 1, 0, 0, 0, 0, 0, 0, 0, 0	1, 1, 1, 1, 1, 1, 1, 1, 1, 1, 1, 1, 1, 0, 0, 0, 0
0.64	0.77	0.83	1, 1, 1, 1, 1, 1, 1, 1, 1, 1, 1, 1, 0, 0, 0, 0	1, 1, 1, 1, 1, 1, 1, 1, 1, 1, 1, 1, 1, 0, 0, 0	1, 1, 1, 1, 1, 1, 1, 1, 1, 1, 1, 1, 1, 1, 1, 0, 0, 0
1	1	1	1, 1, 1, 1, 1, 1, 1, 1, 1, 1, 1, 1, 1, 1, 1, 1, 1, 1	1, 1, 1, 1, 1, 1, 1, 1, 1, 1, 1, 1, 1, 1, 1, 1, 1, 1	1, 1, 1, 1, 1, 1, 1, 1, 1, 1, 1, 1, 1, 1, 1, 1, 1, 1

Table 15: Details of  $\gamma$  of NeFL on Wide ResNet101\_2

Model size		NeFL-D (Wide ResNet101_2)				
$\gamma$	$\gamma^W$	$\gamma^D$	Layer 1 (128)	Layer 2 (256)	Layer3 (512)	Layer 4 (1024)
0.5	1	0.51	1,1,1	1,1,1,1	1, 1, 1, 1, 1, 1, 1, 0, 0, 0, 0, 0, 0, 0, 0, 0, 0, 0, 0, 0	1,1,0
0.75	1	0.75	1,1,1	1,1,1,1	1, 1, 1, 1, 1, 1, 1, 1, 1, 1, 0, 0, 0, 0, 0, 0, 0, 0, 0, 0	1,1,1
1	1	1	1,1,1	1,1,1,1	1, 1, 1, 1, 1, 1, 1, 1, 1, 1, 1, 1, 1, 1, 1, 1, 1, 1, 1, 1	1,1,1